

CORRELATION BETWEEN EARTH TIDE ANOMALIES AND TECTONIC FEATURES THROUGH HEAT FLOW DATA

M. DE BECKER*, B. DUCARME**, P. MELCHIOR, CH. POITEVIN* and
M. VAN RUYMBEKE.

*Royal Observatory of Belgium
Avenue Circulaire, 3
B-1180 Bruxelles
BELGIUM*

Observed tidal deformations appear to be larger in high heat flow areas and lower in low heat flow areas. Geotectonic interpretation is proposed to explain a correlation coefficient 0.77 between the heat flow values and the gravity tide residues.

As deformações de maré observadas parecem ser maiores em áreas de alto fluxo térmico e menores em áreas de baixo fluxo térmico. Uma interpretação geotectônica é proposta para explicar o coeficiente de correlação de 0.77 entre os valores de fluxo térmico e os resíduos de gravidade associados às marés.

(Traduzido pela Revista)

INTRODUCTION

The earth tides phenomena were mainly known up to now to astronomers, geodesists and gravimetrists: indeed, the tidal gravitational effect is primarily due to the attraction of the Sun and the Moon. However, since the waters move and the "solid earth" is not rigid, these tides cause a redistribution of masses that in itself produces secondary tidal effects, directly through the attraction of the water masses moved by the oceanic tides and indirectly through the flexure of the crust under the variable loading of these water masses. In some areas, like North Eastern Brazil, Melchior et al. (1986), England, Spain or the Pacific Islands, these effects are quite large and can reach sometimes 20 microgals. These "indirect" effects have made oceanographers also more interested in earth tides phenomena.

However geotectonic structures differ in their response to the gravitational attraction of Moon and Sun. These differences, expressed as tidal anomalies, contain a unique information on the mobility of large deep seated lateral inhomogeneities of the Earth. The purpose of this paper is to show that the Earth tides phenomena are also interesting for geotectonicians through a correlation between tidal anomalies and, namely, heat flow.

EARTH TIDES

In 1973, the Royal Observatory of Belgium, cooperating with the International Centre for Earth Tides (ICET), started a "Trans World Tidal Gravity Profile" which is still continuing.

Up to now, 109 temporary tidal gravity stations in Africa, Asia, Australia, South Pacific and South America have been established, Melchior et al. (1984).

Each station is maintained in operation for a period of six months continuous recording with a gravimeter (Geodynamics or LaCoste Romberg), a quartz clock and recorders. On each continent a fundamental station has been established to compare the gravimeters and check the reliability of their calibration with respect to the fundamental station Uccle, Ducarme (1975).

A set of data collected within six months of observation allows the determination of amplitude and phase of nine main tidal waves: four in the diurnal (about 24 hours) band, four in the semi-diurnal (about 12 hours) band, and one in the ter-diurnal (about 8 hours) band.

These observed amplitudes and phases are compared with the corresponding data calculated on the basis of the tidal variation of gravity of a theoretical

* Centre de Géophysique Interne

** Chercheur qualifié - FNRS.

Earth model and the indirect tidal variations of gravity due to attraction and loading by the corresponding oceanic tide.

The theoretical Earth model has been derived by Molodensky and is consisting of an oceanless elastic non-viscous Earth with liquid core.

The Schwiderski (1980) cotidal maps have been proved to be an excellent working standard for the oceanic tides. Indirect effects are evaluated according to the procedure developed by Farrell (1972). The Green's functions are computed for a Gutenberg-Bullen model. Computations using Green's functions derived from more recent Earth's model do not show any significant difference.

The data can be interpreted easily by using the simple vectorial representation given in Fig. 1. In this paper, we will use the results concerning the main twelve-hour tide M₂, essentially because of its large amplitude and its good definition after 6 months of measurements as diurnal waves have zero amplitude at the equator and very small amplitude in tropical areas.

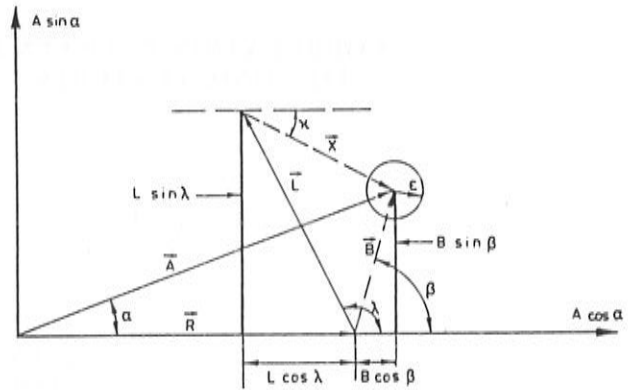


Figure 1 — Determination of tidal residuals. A: observed vector (A: amplitude α : phase); R: tidal vector for an oceanless elastic non-viscous earth with liquid core (R: amplitude, zero phase); L: ocean attraction and loading vector (L: amplitude, λ : phase)

$B = A - R$ (B: amplitude, β : phase).

$X = B - L$ (X: amplitude, χ : phase).

For the wave M₂, the correct scale of this figure should be of the order of: R \approx A \approx 400 nm s⁻² (Europe) to 900 nm s⁻² (equatorial zone)

$\alpha \approx 0^\circ$ to $\pm 5^\circ$

L \approx B \approx 20 to 100 nm s⁻²

instrumental noise

$\epsilon \approx$ nm s⁻² (Europe) to 10 nm s⁻² (equatorial zone)

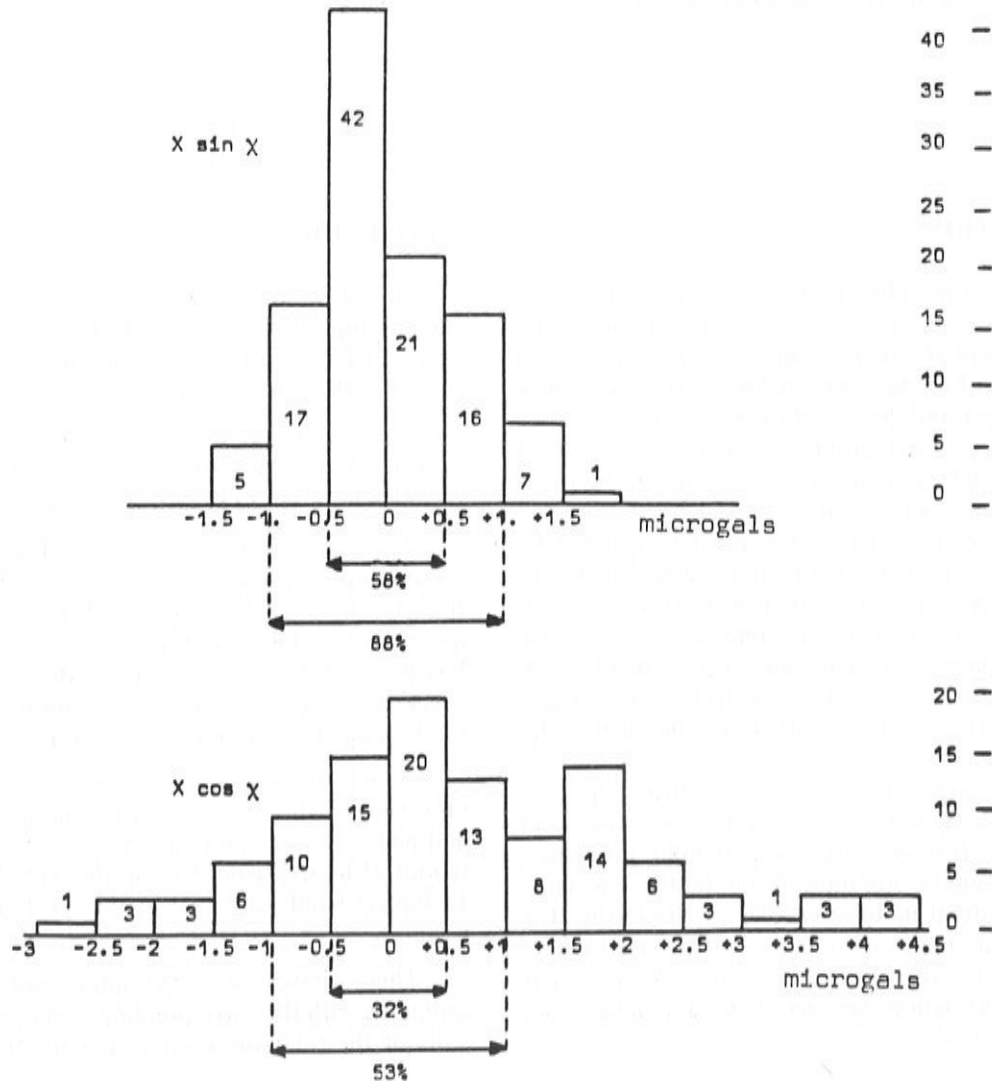


Figure 2 — Histograms of the tidal residues for the twelve-hour tide M₂ (109 tidal gravity stations outside Europe). (a) quadrature ($x \sin \chi$). (b) in-phase ($x \cos \chi$).

The in-phase and quadrature differences between observed and predicted tidal effects are, for most stations, not larger than some tenths of microgals, that is the level of the instrumental noise, Fig. 2.

It thus seems that the observations fit in general rather well with values derived from the theoretical Earth model with a correction for ocean loading calculated from Schwiderski maps.

However, there are some large *in-phase* differences which we will try to elucidate.

PRESENTATION OF THE EXPERIMENTAL DATA

The Data Bank created by the International Center for Earth Tides, Ducarme (1984), is used. As it has been theoretically discussed in Melchior and De Becker (1983) the sine component of the residue vector (X, χ) is clearly independent of the model chosen for the body tides computations e.g. Melodensky (1961) or Wahr (1981). This choice will only affect the R vector and thus only the cosine component (Fig. 1). As already started the computed load vectors (L, λ) are insensitive to the Earth's model at the $0.1 \mu\text{gal}$ level. The histograms of Fig. 2 indicate the consistency of the observations for the sine component while the wide scattering of the cosine component can be attributed to the Earth model.

With respect to this, we discard few observations (13 stations in Fig. 2) for which $|X \sin \chi| > 1 \mu\text{gal}$, considering such large value as due to instrumental effects.

Fig. 3 display the in-phase residues on geographical maps in order to give some global overview of the regional patterns of the tidal residues.

Positive values of $X \cos \chi$ imply an abnormally high response to the tidal variations of gravity while negative $X \cos \chi$ imply an abnormally low response.

GEOTECTONIC INTERPRETATION

From the maps of Fig. 3, it appears that the tidal anomalies are not randomly distributed but seem to indicate local trends.

The chain of positive anomalies runs from the south-western part of Circumpacific mobile belt, from Indonesian archipelago, through New Guinea and Bismarck archipelago up to New Zealand, Fig. 3a.

These are areas of intensive tectonic activity including volcanism and seismicity. The main traits are a hot and relatively shallow asthenosphere, in the lithosphere, tensile stress and deep major faults reaching the top of the asthenosphere.

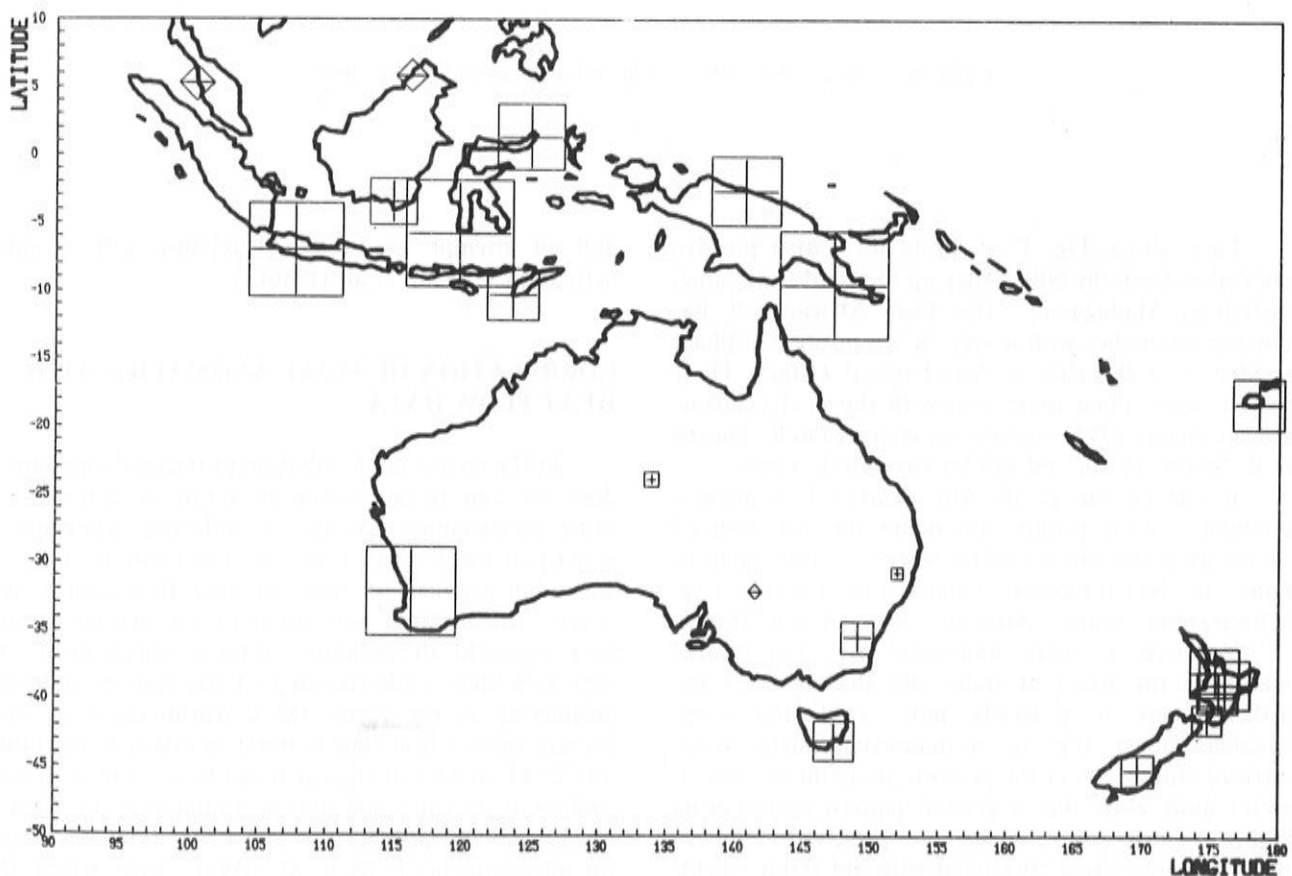


Figure 3a — South East Asia-Australia. Wave M_2 . X, χ cosine component (ICET, 1986).

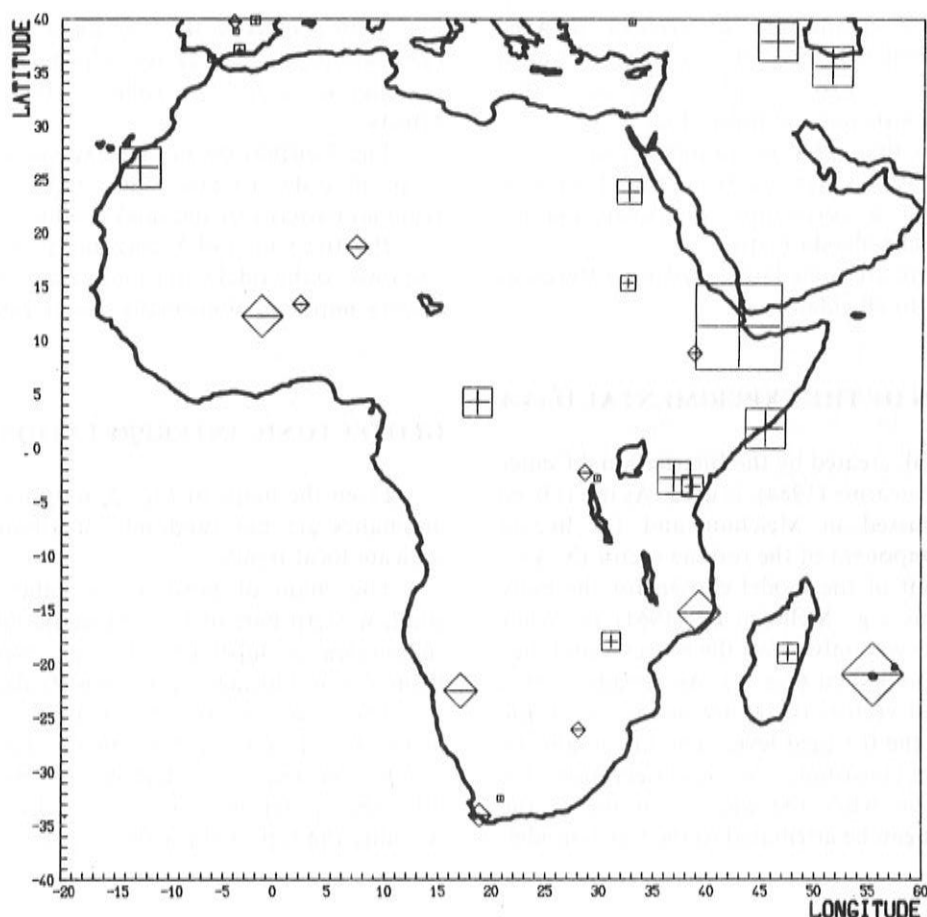


Figure 3b — Africa. Wave M, X, Chi cosine component (ICET, 1986).

East Africa, Fig. 3b, exhibits also rather positive anomalies from the Nile Valley up to the Moçambique, including, Madagascar. The East African rift has positive anomalies with a very strong positive in-phase residue of $4.28 \mu\text{gals}$ in Arta-Djibout (Afar). These regions correspond quite well with those of cenozoic volcanism and rift formation, as described in R. Thorpe & K. Smith (1974), and exhibit also tensile stress.

In Europe, Fig. 3c, the Alps clearly exhibit positive anomalies. Weak positive anomalies are also observed on elevated and superficial basements — Hercynian or older in North-Eastern China and Europe (e.g. Schwarzwald, Vosges, Ardennes, Rhinebergen, Harz).

Negative or weak anomalies are concentrated mainly in the zones of stable old shields where the asthenosphere is generally more cold and deep: Brazilian shield, Fig. 3d, Scandinavian shield, West-African craton. From the geotectonic point of view, it seems quite clear that a general pattern is: opposing regions of negative anomalies and positive anomalies, the first zones being correlated with old stable shields and the others with areas of young high tectonic activity. Correlation with volcanic activity is obvious

and an attempt was made of relation with seismic activity in Yanshin et al. (1986).

CORRELATION OF TIDAL ANOMALIES WITH HEAT FLOW DATA

As the territorial distribution of the tidal anomalies does not seem to be random at all but correlated with some geodynamical parameter reflecting geotectonic activity, it was indicated to relate them with heat flow. The main problem we met with heat flow data is, of course, the unequal repartition of the measurements over the world, the reliability of these measurements as well as a clear understanding of the sources of heat production in the earth. On a worldwide basis the average surface heat flow is about 75 mWm^{-2} . The heat lost at the surface of the earth can be attributed to the cooling of the earth and to heat produced by the decay of radioactive isotopes. The mean heat flow measured for all continents is 56 to 61 mWm^{-2} from which 35 mWm^{-2} can be attributed to the core and the mantle and 23 mWm^{-2} to radioactive isotopes in the crust.

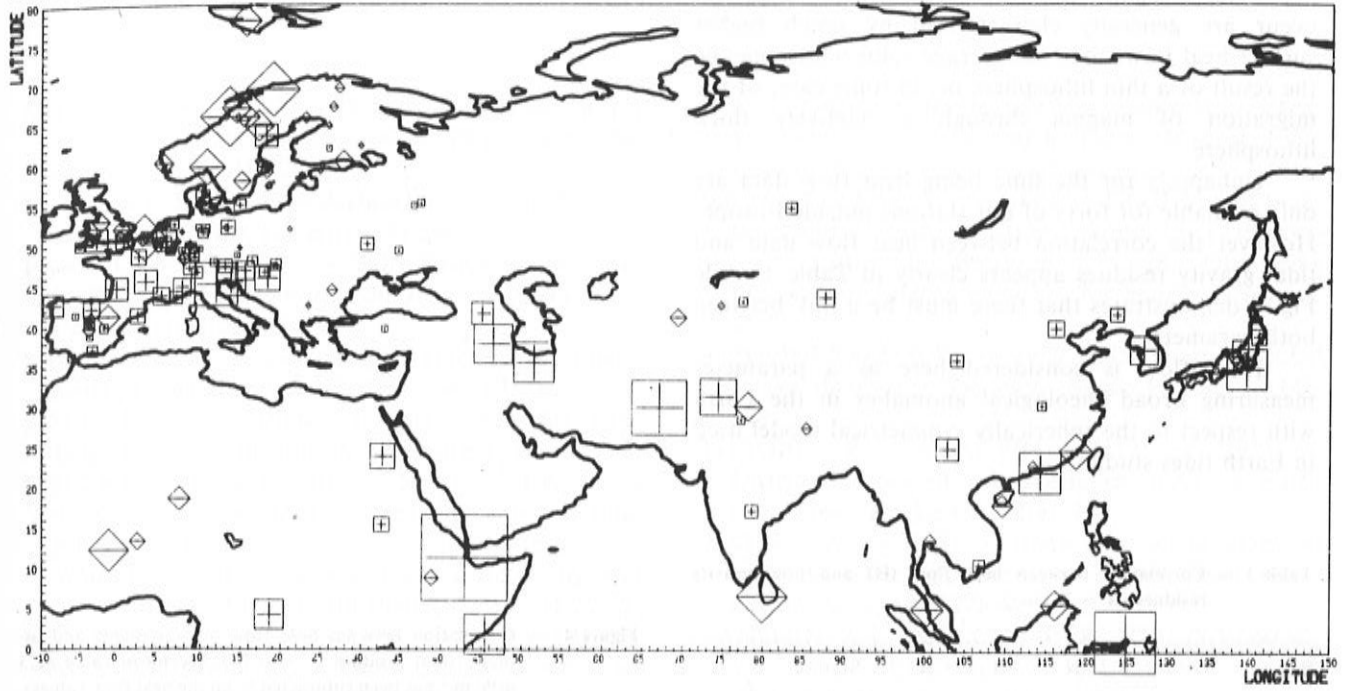


Figure 3c — Europe - Asia. Wave M₂. X, Chi cosine component (ICET, 1986).



Figure 3d — South America. Wave M₂. X, Chi cosine component (ICET, 1986).

Plate margins and other areas where volcanism occur are generally characterized by much higher surface heat flows than the average value which may be the result of a thin lithosphere or, in some case, of the migration of magma through a relatively thick lithosphere.

Unhappily for the time being heat flow data are only available for forty of our stations outside Europe. However the correlation between heat flow data and tidal gravity residues appears clearly in Table 1 while Fig. 4 demonstrates that there must be a link between both parameters.

Heat flow is considered here as a parameter measuring broad rheological anomalies in the Earth with respect to the spherically symmetrical model used in Earth tides studies.

Table 1 — Correlation between heat flow (H) and tidal gravity residues (R = X cos χ).

Region	N	H	R	Station
Niger	3399	20	-1.08	Arlit
Niger	3400	20	-0.66	Niamey
Canada/N.W.T.	6811	25	-0.30	Alert
Burkina Faso	3325	30	-1.93	Ouagadougou
Canada/Ontario	6803	30	-0.24	Ottawa
Canada	6804	42	-0.44	Holland Mills
Philippines	4010	42	-0.41	Baguio
Philippines	4011	42	-0.95	Manila
USSR/UZBEL	1270	42	-0.66	Tashkent
North Borneo	2555	45	-1.30	K. Kinabalu
USSR/Kazakh	1293	46	-0.19	Talgar
USSR/Kirghiz	1280	48	-0.17	Frunze
South Africa	3807	50	-0.96	Stellenbosch/Cape
South Africa	3801	50	-0.56	Johannesburg
USA	6339	50	0.22	Pittsburgh 1/2
Australia/W.A.	4211	50	4.03	Perth
Japan/Hokaido	2897	51	-0.31	Memambetsu
Canada	6807	59	0.15	Halifax
Indian Shield	2402	59	0.43	Hyderabad
New Zealand N	4400	63	2.12	Hamilton
Australia/Central	4209	63	0.44	Alice Springs
Australia/Queensland	4207	65	1.38	Charters Towers
Japan	2823	69	0.04	Kyoto
Japan	2877	70	0.27	Tokyo
Kenya	3031	73	0.87	Voi
Kenya	3030	73	1.47	Nairobi
Pakistan	2352	74	1.63	Peshawar
Iran	2202	75	1.80	Tabriz
Japan	2847	78	0.52	Mizusawa
Somalia	3020	80	1.87	Mogadiscio
New Zealand	4402	83	1.71	Ruapehu
Iran	2201	88	1.86	Teheran
USA/CALIF	6024	90	0.45	Pinon Flat
Australia/N.T.	4210	96	2.90	Darwin
Australia	4206	100	1.30	Canberra
Fiji	4460	101	2.22	Suva
Korea S	2750	110	1.20	Seoul
Australia/Tasmania	4220	110	1.70	Hobart
New Zealand	4401	128	2.16	Taupo
Afar	3019	150	4.28	Arta Djibouti

H in mW.m^{-2}

R is $X \cos \chi$ in microgal

N station code number

Figure 4 — Correlation between heat flow measurements and in-phase tidal residues ($r = 0.769$, the mean value 62.3 mW.m^{-2} has been subtracted from the heat flow values).

CONCLUSION

The theoretical earth tide deformations have been computed on the basis of the Molodensky model I, Molodensky (1961), which is a simple spheroidal symmetric structure of the Earth: the mantle comprises 4 layers for which the values of ρ , μ/ρ and $(\lambda + 2\mu)/\rho$ are fixed (λ and μ being the Lamé parameters and ρ the density), Melchior (1982).

The elastic behavior of the mantle is thus described through μ and λ in a rather simple way but more sophisticated spheroidal symmetric models do not give significant differences. Lateral heterogeneities should be introduced in the model because spheroidal symmetric models fail in regions with strong tectonic character like cratons, volcanic areas, subduction zones etc... which are generally linked to deep mass anomalies. Moreover, an increase in temperature can indeed decrease the local rigidity modulus μ and produces a greater tidal deformations.

Test computations have shown that the oceanic loading effect on the vertical Earth tide component is quite insensitive to the chosen elastic Earth parameters. The anomalies we found cannot be attributed to a bad modelization of loading effects.

The best correlation with heat flow data occurs where there is a drastic tectonic anomaly with a deep rooted origin (hot spot, subduction, craton). In these areas where the earth mantle is more superficial and the lithosphere more "mobile", the Tidal anomalies are generally positive while above a cold and deep asthenosphere with an old thick lithosphere the residues are negative.

REFERENCES

- DUCARME, B. — 1975 — A fundamental station for trans-world tidal gravity profiles. *Phys. Earth Planet. Inter.*, **11**:119-127.
- DUCARME, B. — 1984 — A Data Bank for Earth Tides. *Bull. Inf. Marées Terrestres*, **91**:5963-5980.
- FARREL, W.E. — 1972 — Deformation of the Earth by Surface Loads. *Reviews of Geophysics and Space Physics*, vol. 10, 3:761-797.
- MELCHIOR, P. — 1982 — The Tides of the Planet Earth. Pergamon Press. 2nd ed., 641 PP.
- MELCHIOR, P. — 1986 — Internal geophysics at the Belgian research institutions. *First Break*, vol. 4, n° 5.
- MELCHIOR, P. & DE BECKER, M. — 1983 — A discussion of world-wide measurements of tidal gravity with respect to oceanic interactions, lithosphere heterogeneities, Earth's flattening and inertial forces. *Phys. Earth Planet. Inter.*, **31**:27-53.
- MELCHIOR, P., DUCARME, B., VAN RUYMBEKE, M. & POITEVIN, C. — 1984 — Trans World Tidal Gravity profiles. *Observatoire Royal de Belgique. Bull. d'Observation: Marées Terrestres*. Vol. V, fasc. 1, 102 pp.
- MELCHIOR, P., POITEVIN, C., DUCARME, B., VAN RUYMBEKE, M., GEMAEL, C. & RATTON, E. — 1986 — Tidal Gravity Measurements in Brazil. 10th Int. Symp. on Earth Tides, Madrid 1985. Consejo Sup. Invest. Cientificas, Madrid: 177-188.
- MOLODENSKY, M.S. — 1961 — The theory of nutations and diurnal earth tides. *Comm. de l'Observatoire Royal de Belgique n° 188*, Quatrième Symposium International sur les marées terrestres: 25-56.
- SCHWIDERSKI, E.W. — 1980 — On charting global Ocean tides. *Rev. Geophys. Space Physics* **18**:243-268.
- THROPE, R.S. & KEVIN SMITH — 1974 — Distribution of Cenozoic Volcanism in Africa. *Earth and Planet. Sc. Letters* **22**:91-99.
- WAHR, J.M. — 1981 — Body tides on an elliptical rotating elastic and oceanless earth. *Geoph. J.R. Astron. Soc.*, **64**:677-704.
- YANSHIN, A.L., MELCHIOR, P., KEILIS-BOROK, V.I., DE BECKER, M., DUCARME, B. & SADOVSKY, A.H. — 1986 — Global distribution of tidal anomalies and an attempt of its geotectonic interpretation. 10th Int. Symposium on Earth Tides, Madrid 1985. Consejo Sup. Invest. Cientificas, Madrid: 739-755.